Quad-Ridged Conical Horn Antenna for Wideband Applications

A. R. Mallahzadeh, A. A. Dastranj, S. Akhlaghi

Faculty of Engineering, Shahed University, Tehran, Iran

Received 13 March 2008; accepted 29 December 2008

ABSTRACT: This article presents a quad-ridged conical horn antenna with high gain and low side lobe level for broadband applications. To the best of authors' knowledge, the proposed structure presented in this article is completely new. The designed antenna introduces a low VSWR, which is lower than 2.2 for the frequency range of 8–18 GHz, and simultaneously achieves high gain as well as dual-polarizations with high isolation between the corresponding excitations. The common impedance exponential tapering is used at the flare section of the horn, and a coax to waveguide transition, namely quadruple-ridged circular waveguide, with a conical cavity is used to improve the VSWR. The proposed antenna structure is designed and simulated by two well established packages, namely the CST microwave studio and the Ansoft HFSS, showing there is a close agreement between the results obtained by the aforementioned softwares. © 2009 Wiley Periodicals, Inc. Int J RF and Microwave CAE 19: 519–528, 2009.

Keywords: quad-ridged conical horn antenna; quadruple-ridged circular waveguide; ridge; conical cavity back

I. INTRODUCTION

Horn antennas are widely used for various applications such as radar, satellite tracking systems, reflector feeds, EMC testing, electronic warfare, standard measurement equipment, and detection systems [1–3]. These numerous applications are due to some features such as wide bandwidth, relatively high gain, and directivity performance, which the Horn antennas inherently yield [4, 5].

The idea of using ridges in waveguides was adopted in horns for the first time by Walton and Sundberg [6], and then completed by Kerr in the early 1970's, when they suggested the use of a feed horn launcher whose dimensions were found experimentally [7]. To extend the maximum practical bandwidth of a horn, ridges are introduced in the flare section of the conical horn antenna. This is commonly done in waveguides to increase the cutoff frequency of the higher order modes and thus expands the single-mode range before higher order modes occur [8–10]. Moreover, when quadruple-ridge is used in a circular waveguide, the cutoff frequency of the TE21L mode becomes close to the TE11 mode resulting in an increase in bandwidth between the TE11 and TE10 modes [11].

To have a single polarization, double ridges can be used inside the horn antenna. Also, an E-sectoral horn antenna for broadband application using a double-ridge is addressed in [12, 13]. A detailed investigation on 1–18 GHz broad-band pyramidal double-ridged horn (DRH) antenna is reported in [14]. In [15], a broadband pyramidal DRH antenna for the operating frequency of 1–14 GHz is presented. An improved design for the double-ridged pyramidal

Correspondence to: A. R. Mallahzadeh; e-mail: mallahzadeh@shahed.ac.ir

DOI 10.1002/mmce.20374

Published online 26 June 2009 in Wiley InterScience (www.interscience.wiley.com).

horn antenna is addressed in [16]. Another design for the double-ridged pyramidal horn antenna in the frequency range of 1–18 GHz with a refined feeding section is reported in [17], where several modifications are made in the structure of a conventional DRH antenna to overcome the fluctuation in the radiation pattern at higher frequencies.

Dual polarized antennas are commonly used in radar systems, electronic counter measurement, and EMC applications. To have dual polarizations, in [18] a five layered polarizer at the aperture of the DRH antenna is introduced. A dual-polarized quad-ridged pyramidal horn antenna is reported in [19]. Recently, a new dual-polarized broadband horn antenna over the frequency range of 2–26.5 GHz with a VSWR lower than 3.1 is reported in [20], wherein a novel technique for transition between coax to quadruple-ridged waveguide is introduced to reduce the return loss.

In this article, a dual-polarized conical horn antenna based on the quadruple-ridged circular waveguide for the frequency range of 8–18 GHz is designed. To improve the VSWR (lower than 2.2), a conical cavity back is used.

Furthermore, the proposed antenna presents an isolation >21 dB over the operating frequency. Moreover, a new technique to design the flare section is presented. The proposed antenna when compared with the conventional quad-ridged pyramidal horn antennas introduced in [20], yields lower side lobe level (SLL), higher gain, lower VSWR, and lower cross polarization. The proposed quad-ridged conical horn antenna is simulated by two established packages, namely the Ansoft HFSS, which is based on the finite element method, and the CST microwave studio, which is based on the finite integral technique.

II. DESCRIPTION OF THE ANTENNA CONFIGURATION

The proposed antenna structure is shown in Figure 1. The overall length of the designed antenna and the radius of the horn aperture are 77 and 31.6 mm, respectively. The designed antenna contains three main parts: a quadruple-ridged circular waveguide, a conical cavity back, and finally the flare section with tapered quadruple-ridges. In what follows, the detailed design for the aforementioned parts will be described.

A. Design of the Quadruple-Ridged Circular Waveguide

The quadruple-ridged circular waveguide and a conical cavity back are the two main parts of the coax to waveguide transition. The quadruple-ridged circular waveguide is a circular waveguide which is loaded by four ridges. In the circular quadruple-ridged waveguide, the lowest modes are TE11, TE21, TE10, and TE31, respectively. The TE21 mode, splits into TE21L and TE21U. The TE21L is evolved from two in-phase TE21 modes, each polarized in one of two orthogonal directions, in a circular waveguide. The TE21U is evolved from two antiphase TE21 modes in a circular waveguide. The TE11 is a symmetrical mode which always represents the lowest mode in the circular waveguide, thus serves as the fundamental propagation mode. The TE21 and TE10 mode represent the two lowest odd modes. Contrary to being in a single or double-ridged circular waveguide, the TE21L mode is not only the second lowest mode, but also has a cutoff frequency very close to that of the TE11 mode, when the ridges are heavily loaded. The TE31 is the second-lowest symmetrical mode which has a much higher cutoff frequency than the TE10 mode [11].

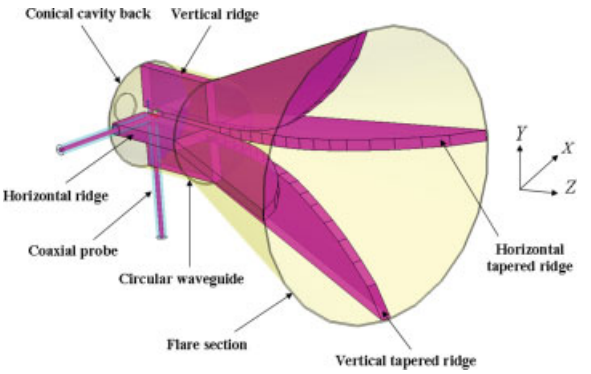

Figure 1. Configuration of the proposed quad-ridged conical horn antenna. [Color figure can be viewed in the online issue, which is available at www.interscience.wiley.com.]

For single-mode operation, an increase of the bandwidth between the TE11 and the TE10 modes and an impedance matching to coax (50 Ω) can be obtained by loading ridges with a very small gap. To do this, at first a two port quadruple-ridged circular waveguide without coaxial probes (Fig. 2) is simulated for the TE11 mode (the single mode) in the operating bandwidth. The height, width, and spacing of the designed ridges are, respectively, $h = 9.1$ mm, $w = 2.4$ mm, and $s = 3.8$ mm. Also, the radius and the overall length of the circular waveguide are $r = 11$ mm and $l = 20$ mm, respectively. The S12 parameters of the TE11 and TE10 modes in circular waveguide versus the frequency are shown in Figures 3

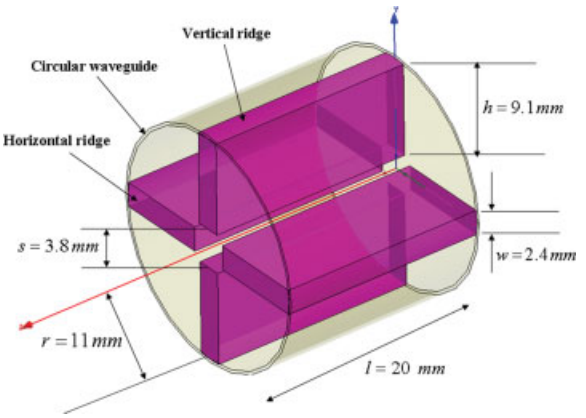

Figure 2. Two port quadruple-ridged circular waveguide without coaxial probes. [Color figure can be viewed in the online issue, which is available at www.interscience.wiley.com.]

and 4. Figure 3 shows that the lowest mode (TE11) is the fundamental propagation mode in the waveguide, because the corresponding S12 parameter is 0 dB. TE21L mode is close to the TE11 in cutoff frequency. This fact distinguishes a quadruple-ridged circular waveguide significantly from a single- or double-ridged circular waveguide. However, if the TE21L mode is sufficiently suppressed or not excited, the frequency bandwidth between the TE11 and the TE10 can be very large [11]. In Figure 4, we observe that the higher order mode, TE10, cannot propagate in the circular waveguide, because the S12 parameter is much lower than 0 dB. The characteristic impedance of the fundamental propagation mode, TE11, versus frequency is shown in Figure 5, which is obtained by the Ansoft HFSS. As is inferred from Figure 5, the characteristic impedance varies between 51.1 Ω (8 GHz) and 50.2 Ω (18 GHz), which shows there is a good impedance matching between the

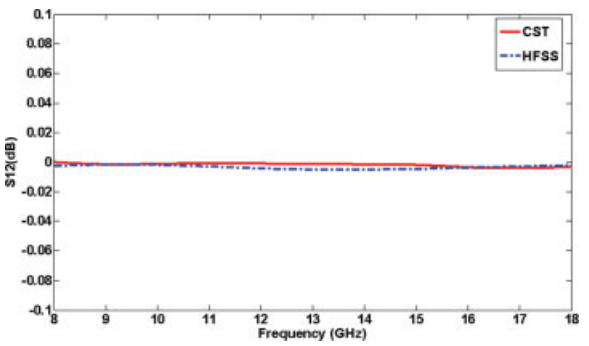

Figure 3. S12 parameter of the propagation mode (TE11 mode) versus frequency. [Color figure can be viewed in the online issue, which is available at www.interscience.wiley.com.]

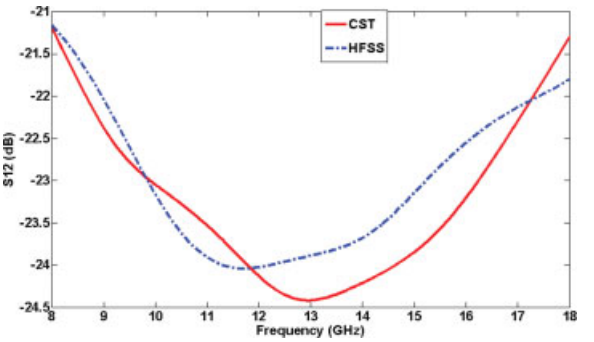

Figure 4. S12 parameter of the nonpropagation mode (TE10 mode) versus frequency. [Color figure can be viewed in the online issue, which is available at www.interscience.wiley.com.]

coaxial line and quadruple-ridged circular waveguide for the entire frequency bandwidth.

B. Coaxial to Quadruple-ridged Circular Waveguide Transition

It is necessary to use a transition between the two coaxial probes and the quadruple-ridged circular waveguide. Two coaxial probes are used for the vertical polarization and the horizontal polarization. The transition between the coaxial probes and the quadruple-ridged circular waveguide plays an important role for the isolation and the return loss. To have a low VSWR, the cavity back dimensions as well as the distance of the probe from the edge of the corresponding ridge should be optimized. Moreover, the results show that the distance between the probes and the edge of the ridges affects the antenna gain and the main lobe of the radiation pattern. Numerous simulations have been made to optimize the transition parameters. As is shown in Figure 6a, the shield of the coaxial probe is connected to the lower ridge and the inner conductor is connected to the upper ridge by passing a tunnel through the lower ridge. The second coaxial probe follows the same procedure. As is shown in Figure 6b, the horizontal ridges are shorter than the vertical ridges, because there should be a gap between the probes. This is due to the fact that the probes should be placed at the end of the ridges to have a low VSWR. The gap between the horizontal and the vertical ridges is optimized to $d = 0.85$ mm (Fig. 6b).

A cavity back is commonly used to improve the VSWR of the coax to quad-ridged waveguide transition. As are shown in Figures 7 and 8, two configurations for the cavity back is used, a cylindrical and a conical cavity back. The former has a VSWR not

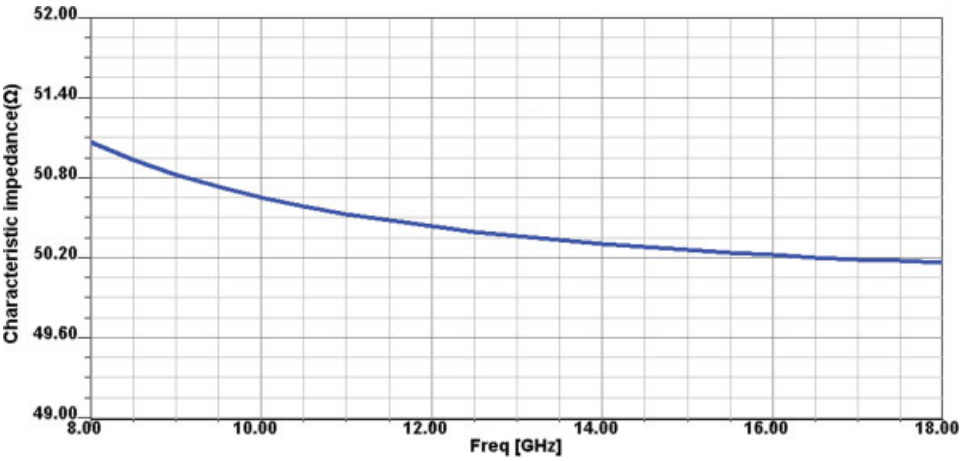

Figure 5. The characteristic impedance of the propagation mode (TE11 mode) versus frequency (simulated by Ansoft HFSS). [Color figure can be viewed in the online issue, which is available at www.interscience.wiley.com.]

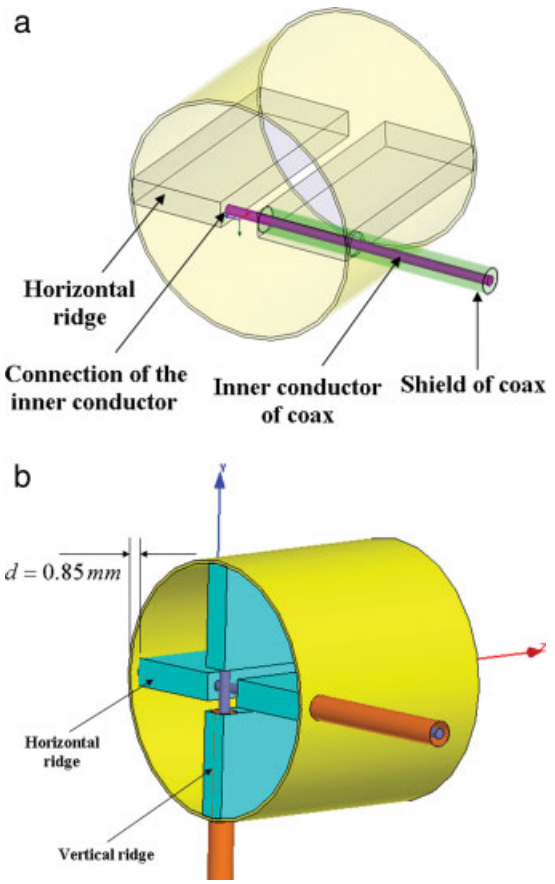

Figure 6. (a) Coaxial probe entrance to the horizontal ridges in the waveguide transition and (b) the vertical and the horizontal ridges in the waveguide transition with coaxial probes. [Color figure can be viewed in the online issue, which is available at www.interscience.wiley.com.]

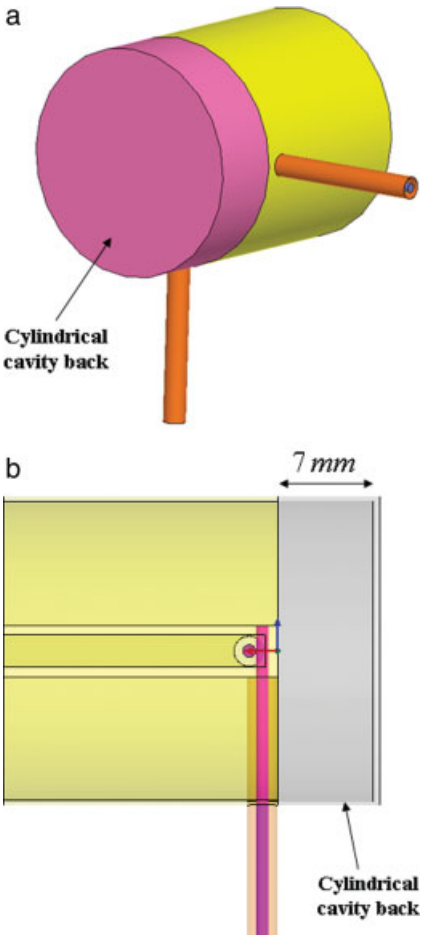

Figure 7. Cylindrical cavity back in the waveguide transition: (a) overall view and (b) side view. [Color figure can be viewed in the online issue, which is available at www.interscience.wiley.com.]

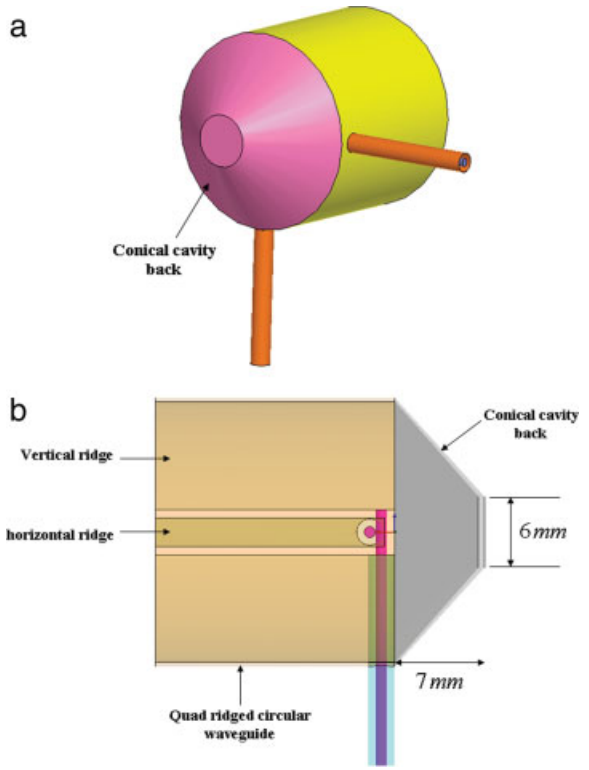

Figure 8. Conical cavity back for return loss improvement in the waveguide transition: (a) overall view and (b) side view. [Color figure can be viewed in the online issue, which is available at www.interscience.wiley.com.]

greater than 2.6, as well as an isolation <16 dB, which may not be adequate in certain applications. The latter, however, will enhance the VSWR as well as the isolation.

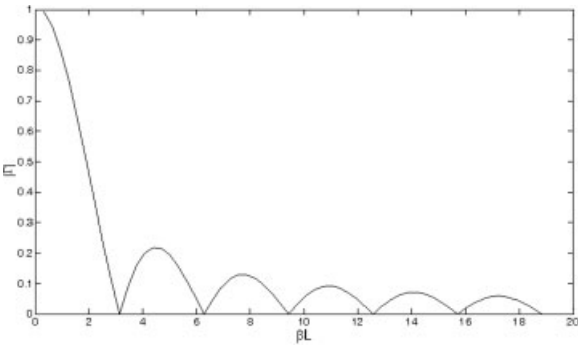

Figure 9. Magnitude of the reflection coefficient versus βL.

C. Determination of the Axial Length and Aperture Size of the Designed Conical Horn

The axial length of the horn opening (flare section) should satisfy the inequality $L > \lambda$, where $\lambda = 2\pi/\beta$ and β is the wave number [6]. For the desired gain, ~14–15 dB, at center frequency (13 GHz), the aperture size is determined from the simulation of the horn antenna in the absence of the ridges. The radius of the horn aperture is found to be 31.6 mm and the length of the flare section is 50 mm.

D. Design of the Tapered Part

The design of the tapered section is the most significant part in the antenna design. The exponential tapered ridges transform the impedance of the guide from 50 Ω at the feeding point (quadruple-ridged cir-

TABLE I. The Design Detail Dimensions of the Tapered Part (at 13 GHz)

Waveguide Number	Radius of the Waveguide Aperture (mm)	Characteristic Impedance (Ω)	Height of the Tapered Ridge (mm)	Length of the Tapered Ridge (mm)
1	11.0	50.0	9.1	3
2	12.2	56.4	10.2	3
3	13.5	63.7	11.3	3
4	14.7	71.8	12.3	3
5	15.9	81.1	13.1	3
6	17.2	91.0	13.8	3
7	18.4	103.2	14.3	3
8	19.7	116.5	14.5	3
9	20.9	131.5	14.4	3
10	22.1	148.4	13.9	3
11	23.4	167.4	13.2	4
12	25.0	196.7	11.9	4
13	26.7	231.1	10.3	4
14	28.3	271.5	7.9	4
15	29.9	318.9	5.2	4

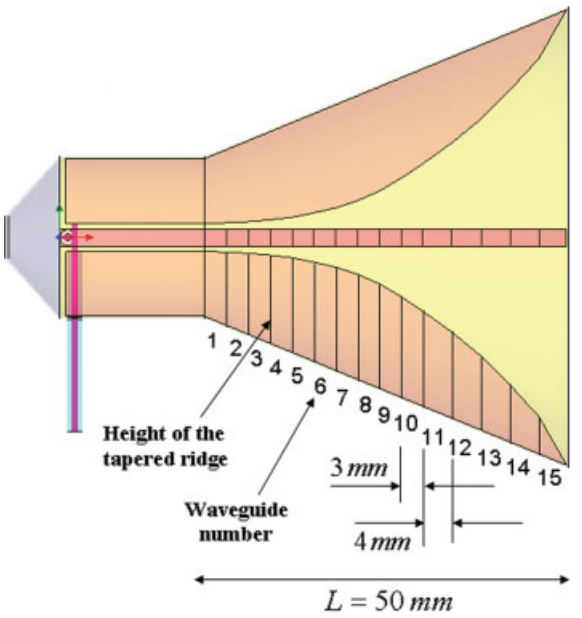

Figure 10. The quad-ridged conical horn antenna including 15 smaller waveguides of different height. [Color figure can be viewed in the online issue, which is available at www.interscience.wiley.com.]

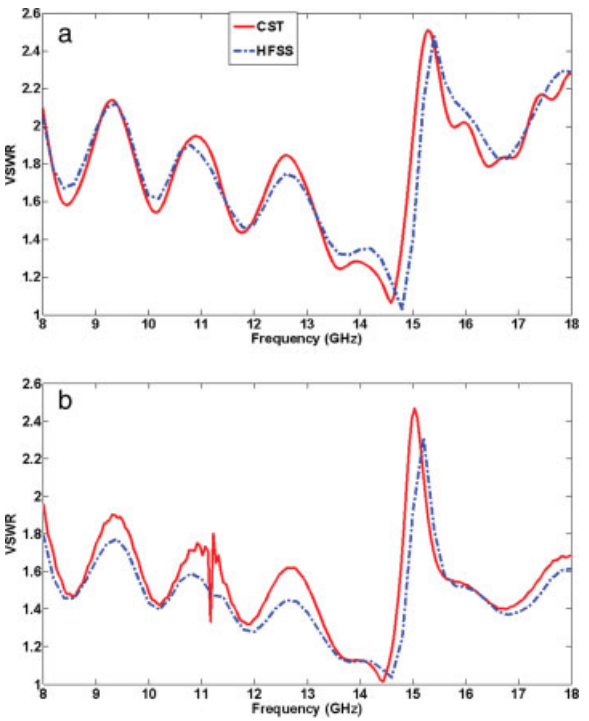

Figure 11. Simulated VSWR of the quad-ridged conical horn antenna with cylindrical cavity back: (a) VSWR of port 1 and (b) VSWR of port 2. [Color figure can be viewed in the online issue, which is available at www.interscience.wiley.com.]

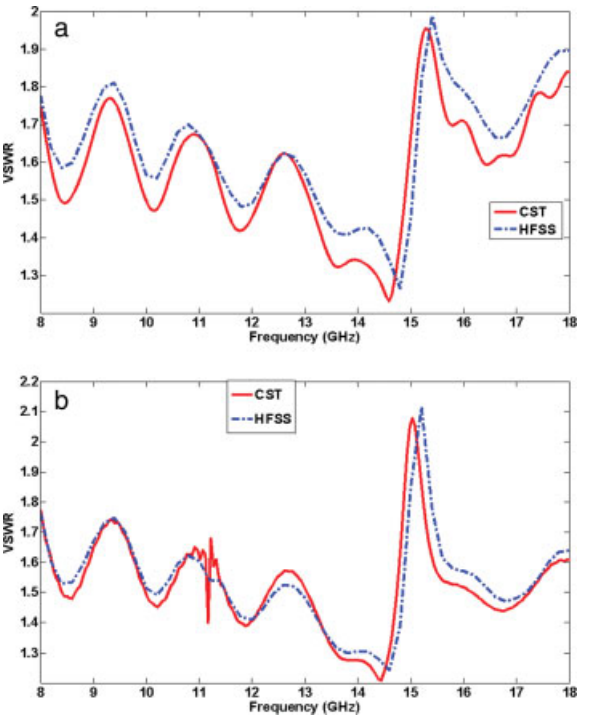

Figure 12. Simulated VSWR of the proposed quad-ridged conical horn antenna with conical cavity back: (a) VSWR of port 1 and (b) VSWR of port 2. [Color figure can be viewed in the online issue, which is available at www.interscience.wiley.com.]

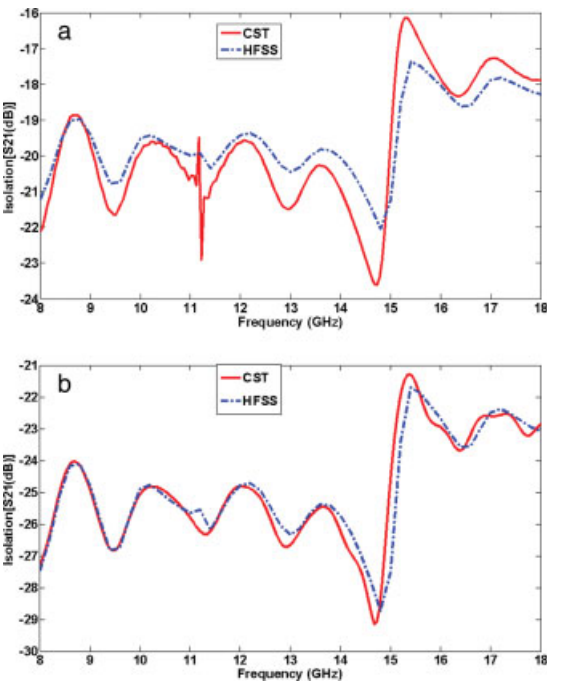

Figure 13. Isolation S12, (a) quad-ridged conical horn antenna with cylindrical cavity back and (b) quad-ridged conical horn antenna with conical cavity back. [Color figure can be viewed in the online issue, which is available at www.interscience.wiley.com.]

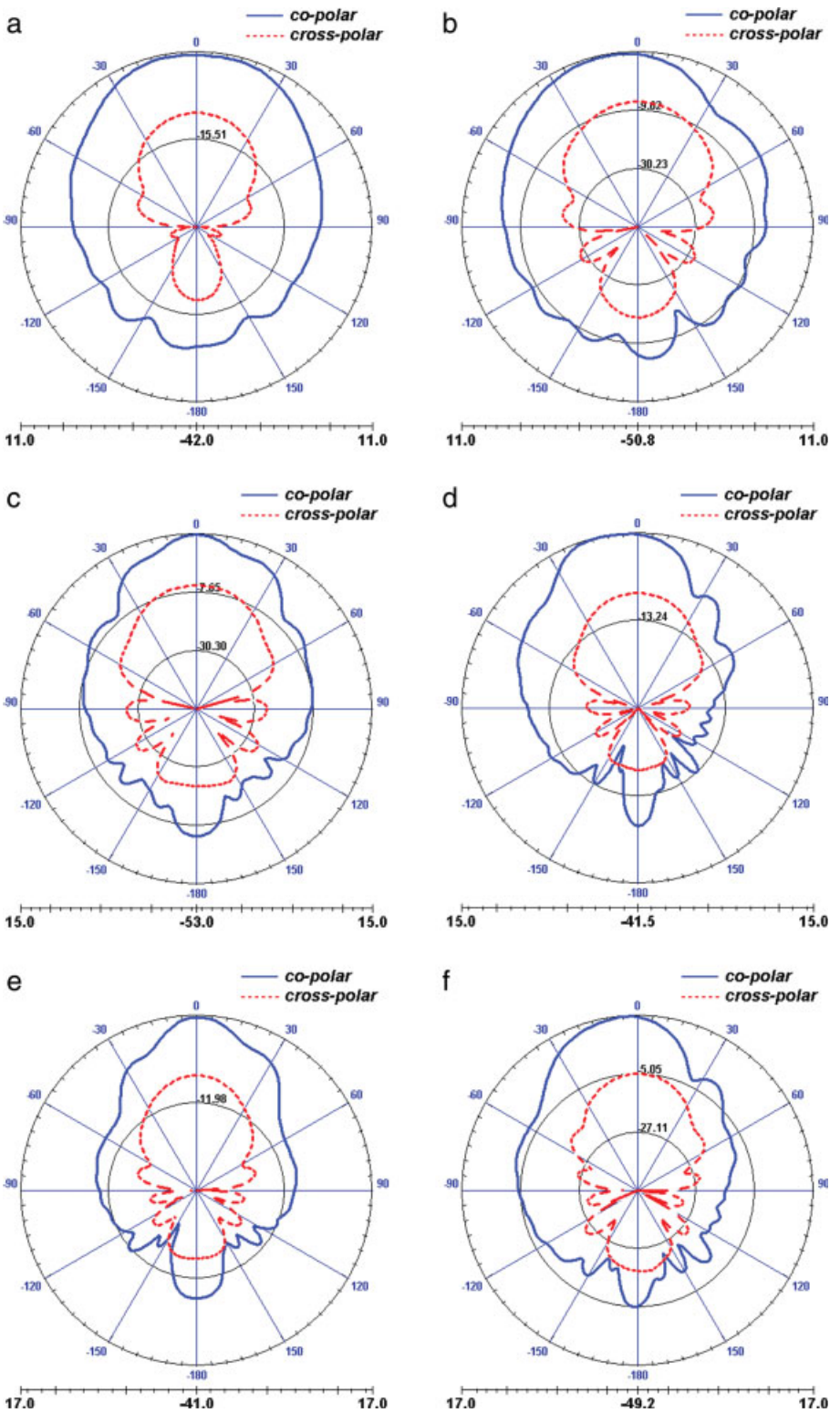

Figure 14. Radiation patterns: (a) E-plane at 8 GHz, (b) H-plane at 8 GHz, (c) E-plane at 13 GHz, (d) H-plane at 13 GHz, (e) E-plane at 18 GHz, and (f) H-plane at 18 GHz. [Color figure can be viewed in the online issue, which is available at www.interscience.wiley.com.]

TABLE II. He Radiation Pattern Characteristics of the Proposed Antenna for E-Planes and H-Planes at Various Frequencies

Frequency (GHz)	Plane	Maximum Magnitude of the Cross Polar (dB)	SLL (dB)	HPBW (deg)
8	E	−7.6	−14.9	60.1
8	H	−6.7	−14.6	49.9
13	E	−5.6	−18.2	20.1
13	H	−4.2	−18.4	33.2
18	E	−2.7	−21.5	17.9
18	H	−4.9	21.9	29.3

cular waveguide) to 377 Ω at the aperture of the horn antenna [6]. The impedance variation in the tapered part is as follows:

$$Z(y) = Z_0 e^{ky}, \quad (0 \le y \le L), \tag{1}$$

where y is the distance from the waveguide aperture and L is the axial length of the horn opening (flare section), which is determined in Section C (with L = 50 mm). Then, k is obtained from the following equation [21]:

$$k = \frac{1}{L}\ln\left(\frac{Z_L}{Z_0}\right), \tag{2}$$

where Z_0 and Z_L are, respectively, the characteristic impedances of quadruple-ridged circular waveguide and free space. Figure 9 depicts the reflection coefficient of exponential taper line, Γ, versus βL.

To derive dimensions of the flare section regarding the exponential tapering, the following algorithm is proposed:

The axial length of the flare section (L) is divided into 15 subsections, resulting 15 smaller quadruple-ridged circular waveguides. Each corresponding aperture size is obtained from the main conical horn antenna structure. Then, the height of each quadruple-ridged circular waveguides should be optimized (the Ansoft HFSS is used), such that the corresponding characteristic impedance holds according to eq. (1). The designed details for the corresponding dimensions of the tapered section at 13 GHz are given in Table I. Once the heights of the ridges are obtained, they are merged together to shape the flare section of the horn antenna (Fig. 10).

III. SIMULATION RESULTS

The designed antenna as is discussed in the preceding sections, are analyzed by two commercially available software packages, the HFSS and the CST softwares. The simulation results show that there is a good agreement between the results obtained by two aforementioned softwares. This confirms the accuracy of simulations.

The VSWR of the quad-ridged conical horn antenna with cylindrical cavity back is presented in Figure 11. It can be seen that the VSWR is <2.6 for the frequency range of 8–18 GHz for both of excitations. Also, the VSWR of the proposed quad-ridged conical horn antenna with conical cavity back is presented in Figure 12, showing the resulting VSWR is <2.2 for both of excitations.

The isolation, S12, between the two coaxial ports is better than 16 and 21 dB, respectively, for the cylindrical and the conical cavity back (Figs. 13a and 13b).

Figure 14 shows the copolar and the cross-polar far-field radiation patterns in the E-plane (y-z plane) and the H-plane (x-z plane) at 8, 13, and 18 GHz for the proposed antenna with conical cavity back, showing low-cross polarization, low SLL, low-back lobe, high gain, and satisfactory far-field radiation pattern. Table II provides main characteristics of the proposed antenna, such as the maximum magnitude of the cross polar, SLL, and half power beam width in both the E-plane and the H-plane at various frequencies. Compared with the proposed conventional quad-ridged pyramidal horn antennas in [20], the proposed antenna (with lower aperture size) gives the better SLL, gain, isolation, and cross polarization. The radiation patterns are shown in Figure 14.

The proposed antenna gain versus frequency is shown in Figure 15. It can be seen that the antenna gain increases as the frequency increases. The maximum value of gain is around 16.2 dB and occurs at the end of the operating frequency band (18 GHz).

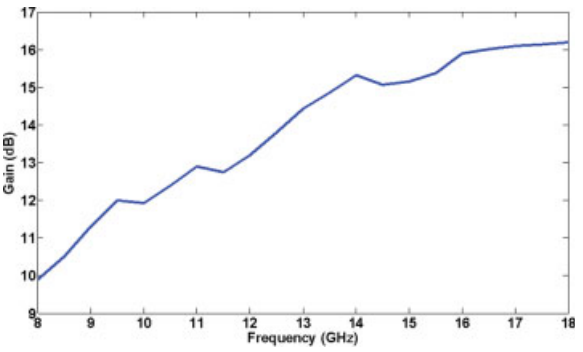

Figure 15. Gain versus frequency for the proposed quad-ridged conical horn antenna. [Color figure can be viewed in the online issue, which is available at www.interscience.wiley.com.]

Simulation results show that the gain and the radiation pattern are the same for both of the horizontal and the vertical polarizations.

IV. CONCLUSION

In this article, a novel dual-polarized quad-ridged conical horn antenna is proposed for the frequency band of 8–18 GHz. A conical cavity back is used to enhance the VSWR (<2.2) and also the isolation (>21 dB). Moreover, the proposed antenna yields high gain, dual-polarizations, low SLL, low-cross polarization, and satisfactory far-field radiation pattern. To verify the accuracy of the simulated results, two commercial software packages, the HFSS and the CST are used. Compared with the conventional quad-ridged pyramidal horn antennas, the proposed antenna achieves better radiation pattern, which makes it suitable to be used in various applications.

REFERENCES

1. V. Venkatesan and K.T. Selvan, Rigorous gain measurements on wide-band ridge horn, IEEE Trans Electromagn Compat 48 (2006), 592–594.
2. M. Abbas-Azimi, F. Arazm, and R.F. Dana, Design and optimization of a high frequency EMC wideband horn antenna, IET Microwave Antennas Propag 1 (2007), 580–585.
3. A. Hizal and U. Kazak, A broadband coaxial ridged horn antenna, Proc 19th Eur Microwave Conf, Turnbridge Wells, UK, 1989, pp. 247–252.
4. W.L. Barrow and L.J. Chu, Theory of the electromagnetic horn, Proc IRE 27 (1939), 51–64.
5. F.F. Dubrovka, G.A. Yena, P.Y. Stepanenko, and V.M. Tereschenko, Ultra wideband double ridged horn with rectangular aperture, Int Conf Antenna Theory Tech, Seuastopol, Ukraine, 9–12 September 2003, pp. 590–593.
6. K.L. Walton and V.C. Sundberg, Broadband ridged horn design, Microwave J 4 (1964), 96–101.
7. J.L. Kerr, Short axial length broad-band horns, IEEE Trans Antennas Propag AP-21 (1973), 710–714.
8. S. Hopfer, The design of ridged waveguides, IRE Trans Microwave Theory Tech MIT-3 (1955), 20–29.
9. S.B. Cohn, Properties of ridged waveguide, Proc IRE 35 (1947), 783–788.
10. D.A. Jarvis and T.C. Rao, Design of double-ridged rectangular wave guide of arbitrary aspect ratio and ridge height, Microwave Antenna Propag IEE Proc 147 (2000), 31–34.
11. W. Sun and C.A. Balanis, Analysis and design of quadruple ridged waveguide, IEEE Trans Microwave Theory Tech 42 (1994), 2201–2207.
12. C. Reig and E. Navarro, FDTD analysis of E-sectoral horn antenna for broadband applications, IEEE Trans Antennas Propag 45 (1997), 1485–1487.
13. R. Bunger, R. Beyer, and F. Arndt, FDTD analysis of E-sectoral horn antennas for broadband applications, IEEE Trans Antennas Propag 47 (1999), 1641–1648.
14. C. Bruns, P. Leuchtmann, and R. Vahldieck, Analysis and simulation of a 1–18 GHz broadband double-ridged horn antenna, IEEE Trans Electromagn Compat 45 (2003), 55–59.
15. M. Botello-Perez, H. Jardon-Aguilar, and I. Ruiz, Design and simulation of a 1 to 14 GHz broadband electromagnetic compatibility DRGH antenna, ICEEE-ICE 2005, 2nd Int Conf Electr Electron Eng, Mexico City, Mexico, September 2005, pp. 118–121.
16. V. Rodriguez, New broadband EMC double-ridged guide horn antenna, R F Des 27 (2004), 44–47.
17. M. Abbas-Azimi, F. Arazm, J.R. Mohassel, and R. Faraji-Dana, Design and optimization of a new 1–18 GHz double ridged guide horn antenna, J Electromagn Wave Appl 21 (2007), 501–506.
18. A.R. Mallahzadeh, A.A. Dastranj, and H.R. Hassani, A novel dual-polarized double-ridged horn antenna for wideband applications, Prog Electromagn Res B 1 (2008), 67–80.
19. H. Lai, R. Franks, D. Kong, D. Kuck, and T. Gackstetter, A broad band high efficient quad ridged horn, Antennas Propag Soc Int Symp 5 (1987), 676–679.
20. Z. Shen and C. Feng, A new dual-polarized broadband horn antenna, IEEE Antenna Wireless Propag Lett 4 (2005), 270–273.
21. D.M. Pozar, Microwave engineering, 3rd ed., John Wiley, New York, 2005.

BIOGRAPHIES

Alireza Mallahzadeh was born in Bushehr, a beautiful city in the south of Iran in 1977. He received the B.S. degree in electrical engineering from Isfahan University of Technology, Isfahan, Iran in 1999 and the M.Sc. degree in electrical engineering from Iran University of Science and Technology, Tehran, Iran in 2001, and the Ph.D. degree in electrical engineering from Iran University of Science and Technology, Tehran, Iran in 2006. He is a member of academic staff, Faculty of Engineering, Shahed University, Tehran, Iran. He has participated in many projects relative to antenna design, which resulted in fabricating different types of antennas for various companies. Also, he is interested in numerical modeling and microwaves.

Aliakbar Dastranj was born in Yasouj, Iran in 1983. He received the B.Sc. degree in electronic engineering from Shiraz University, Shiraz, Iran in 2006, and is currently working toward the M.Sc. degree in electrical engineering at the Shahed University, Tehran, Iran. His research interests include wideband horn antennas, analysis and design of microstrip antennas, broadband monopole antennas, design and modeling of microwave structures, antennas in the RF and microwave range for the wireless communication systems, and electromagnetic theory.

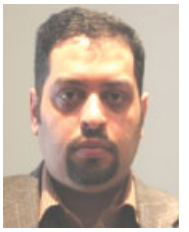

Soroush Akhlaghi was born in Isfahan, Iran. He received the B.A.Sc. degree in electrical engineering from K.N. Toosi University of Technology, Tehran, Iran in 1999, the M.Sc. degree from Amirkabir University of Technology, Tehran, Iran in 2001, and the Ph.D. degree from Iran University of Science and Technology (IUST) in 2007. In 2008, he joined the department of engineering, Shahed University, Tehran, Iran, as an Assistant Professor. In 2005, while working toward his Ph.D., he joined the Coding and Signal Transmission Laboratory, Department of Electrical and Computer Engineering, University of Waterloo, Waterloo, ON, Canada as a Research Assistant. He is currently collaborating with this Laboratory in the area of new emerging Wireless Technologies.